BAMS Article

The Boundary Layer Air Quality-Analysis Using Network of Instruments (BAQUNIN) Supersite for Atmospheric Research and Satellite Validation over Rome Area

Anna Maria Iannarelli, Annalisa Di Bernardino, Stefano Casadio, Cristiana Bassani, Marco Cacciani, Monica Campanelli, Giampietro Casasanta, Enrico Cadau, Henri Diémoz, Gabriele Mevi, Anna Maria Siani, Massimo Cardaci, Angelika Dehn, and Philippe Goryl

ABSTRACT: The Boundary layer Air Quality-analysis Using Network of Instruments (BAQUNIN) supersite is presented. The site has been collecting pollutant concentrations and meteorological parameters since 2017. Currently, BAQUNIN consists of three observation sites located in the city center of Rome (Italy), and in the neighboring semirural and rural areas. To the best of our knowledge, BAQUNIN is one of the first observatories in the world to involve several passive and active ground-based instruments installed in multiple locations, managed by different research institutions, in a highly polluted megacity affected by coastal weather regimes. BAQUNIN has been promoted by the European Space Agency to establish an experimental research infrastructure for the validation of present and future satellite atmospheric products and the in-depth investigation of the planetary and urban boundary layers. Here, the main characteristics of the three sites are described, providing information about the complex instrumental suite and the produced data. The supersite adopts a policy of free sharing of its validated dataset with the community. Finally, the BAQUNIN potential is demonstrated with a case study involving a major fire that occurred in a waste treatment plant near the urban center of Rome, and the consequent investigation of the plume properties revealed by different instruments.

KEYWORDS: Boundary layer; Air quality; In situ atmospheric observations; Profilers, atmospheric; Remote sensing; Surface observations

https://doi.org/10.1175/BAMS-D-21-0099.1

Corresponding author: Annalisa Di Bernardino, annalisa.dibernardino@uniroma1.it

In final form 3 December 2021

AFFILIATIONS: Iannarelli, Mevi, and Cardaci—Serco Italia SpA, Frascati, Rome, Italy; **Di Bernardino, Cacciani, and Siani**—Department of Physics, Sapienza University of Rome, Rome, Italy; **Casadio**—Serco Italia SpA, and EOP-GMQ, ESRIN, ESA, Frascati, Rome, Italy; **Bassani**—Institute of Atmospheric Pollution Research (IIA), National Research Council of Italy (CNR), Monterotondo, Rome, Italy; **Campanelli and Casasanta**—Institute of Atmospheric Sciences and Climate (ISAC), National Research Council of Italy (CNR), Rome, Italy; **Cadau**—Serco Italia SpA, and EOP-GMQ, ESRIN, ESA, Frascati, Rome, and Sardegna Clima Onlus, Fonni, Nuoro, Italy; **Diémoz**—ARPA Valle d'Aosta, Saint-Christophe, Aosta, Italy; **Dehn and Goryl**—EOP-GMQ, ESRIN, ESA, Frascati, Rome, Italy

The amount of people living in urban areas is estimated to be around 50% of the total world's population and this percentage is expected to increase, reaching 68% in the next 30 years (United Nations 2019). Two-fifths of cities with populations of 1–10 million people are located near coastlines (Sterzel et al. 2020). Understanding urbanization trends play a key role in sustainable development and in ensuring a good quality of life for the world population. Atmospheric processes in an urban environment are complex due to the presence of tall buildings, roads, and intersections, capable of limiting both ventilation and pollutants dispersion in the layer of the atmosphere closest to the ground, i.e., in the urban boundary layer (UBL). Moreover, in densely populated cities, air quality is degraded by the presence of anthropogenic gases and particulate matter (PM) that are responsible for threatening the environment and the human health and reducing visibility because of the absorption and scattering of solar and terrestrial radiation. Medium and large urban areas are also affected by peculiar phenomena, such as the urban heat island (UHI) and the urban pollution island (UPI), among others. The former gives rise to the alteration of the thermal balance of the urban region compared to rural surroundings (Nuruzzaman 2015); the latter is defined as the spatial and temporal variation in pollutant concentrations that can be ascribed to the presence of typical urban features and activities (Crutzen 2004). Moreover, the interaction between anthropogenic pollutants and urban green areas is complex and ambivalent as regards the effects on ozone and organic secondary particulate, contributing to the worsening of air quality (Bonn et al. 2018).

The detailed knowledge and the forecast of the urban atmosphere composition and the evolution of urban climate are essential to understand the atmospheric processes occurring at the city scale (Baklanov and Nuterman 2009). The international scientific community is promoting the creation of measurement observatories, named supersites, for which a unique definition has not been established so far. Following Sugiura et al. (2011), a supersite should encompass various research topics, covering an extensive area rather than a single point site, with long-term measurements that should be used synergistically and distributed to the public for the benefit of the entire scientific community. However, none of the listed characteristics is strictly mandatory for the establishment of a supersite.

Among the first supersites ever established were the Lindenberg Meteorological Observatory–Richard Assmann Observatory (MOL-RAO) in upper Bavaria, Germany, inaugurated in 1905 focusing on the experimental exploration and interpretation of the atmosphere's physical structure from the ground up to the stratosphere (www.dwd.de/EN/aboutus/locations/observatories/mol/mol.html, last accessed 18 November 2021), and the Boulder Atmospheric Observatory (BAO) in Colorado, United States, founded in 1977 and in operation until 2016

(Kaimal and Gaynor 1983). This latter site was a milestone for the investigation of the planetary boundary layer (PBL) dynamics, aerosols, greenhouse gases, and the validation of new remote sensing tools (Wolfe and Lataitis 2018). During the last two decades, further supersites have been realized to study clouds in tropical areas [Barbados Cloud Observatory (BCO); Stevens et al. 2016], subarctic environment (Pallas Atmosphere-Ecosystem Supersite; Hatakka et al. 2003), Alpine urban environment [Innsbruck Atmospheric Observatory (IAO); Karl et al. 2020], coastal urban environment [Urban Meteorological Observation System (UMS-Seoul); Park et al. 2017], urban and rural environment [Romanian Atmospheric research 3D Observatory (RADO); Nicolae et al. 2010; National Research Council Institute of Methodologies for Environmental Analysis (CNR-IMAA) Atmospheric Observatory (CIAO); Madonna et al. 2011; Site Instrumental de Recherche par Télédétection Atmosphérique (SIRTA); Zhang et al. 2019], and several environmental conditions (www.arm.gov/, last accessed 18 November 2021).

To the best of our knowledge, urban/coastal environments supersites capable of long-term datasets with high spatial–temporal resolution and good accuracy on the urban environment and, at the same time, on the neighboring semirural and rural areas are rare. In this context, the Boundary layer Air Quality-analysis Using Network of Instruments (BAQUNIN) supersite has been designed with the fundamental objective to fill this gap, i.e., to improve the understanding of urban meteorology driving pollutant dispersion and long-range transport phenomena, as well as to support the validation and calibration of satellite-derived products in urban environments.

This paper describes the environmental context of the BAQUNIN supersite, highlighting the strategic location of the sites, summarizing the main research challenges and the present knowledge gaps filled by the scientific program. Moreover, the main experimental activities and the observatory equipment are presented, with special reference to the customized tools developed for BAQUNIN. An example of the capabilities of BAQUNIN data are shown for one of the first notable cases (e.g., Di Bernardino et al. 2021a,b; Campanelli et al. 2021) captured by the instrumentation since the start of the activities. Finally, possible future perspectives of the supersite are discussed.

The BAQUNIN supersite

Environmental context. The city of Rome has a population of about 2.8 million residents in 1,300 km^2 (www.istat.it/en/censuses/population-and-housing/results). Including the metropolitan area, it reaches 4.3 million citizens, representing one of the most densely populated areas in Europe.

The surrounding region is characterized by complex orography (Fig. 1). The city stretches along the Tiber valley and is surrounded by the mountain chain of the Apennines to the north and by the Alban hills to the south. To the west, the surface slope gently decreases until reaching the coast of the Tyrrhenian Sea, about 27 km away from the city center.

According to the Köppen–Geiger criteria (Peel et al. 2007), the climate in Rome is classified as Csa, i.e., hot summer Mediterranean with hot, dry summers and mild, wet winters. Two different peculiar local orography-related circulation patterns are identifiable: (i) the seabreeze regime due to the proximity of the Tyrrhenian coast (Di Bernardino et al. 2021a), and (ii) the drainage flow in the Tiber valley (Petenko et al. 2011). During the daytime, because of the thermal differences between inland and sea surface, the wind generally blows from the southwest in the coastal area and the city center. Conversely, in the internal areas, the airflow veers to the northeast, due to the prevalence of the drainage circulation that characterizes the Tiber valley.

Commerce and services represent the main economic activities in the area, while there are no large industrial plants near the urban center. This implies that emissions of atmospheric pollutants mainly originate from vehicular traffic and residential heating. In addition to the

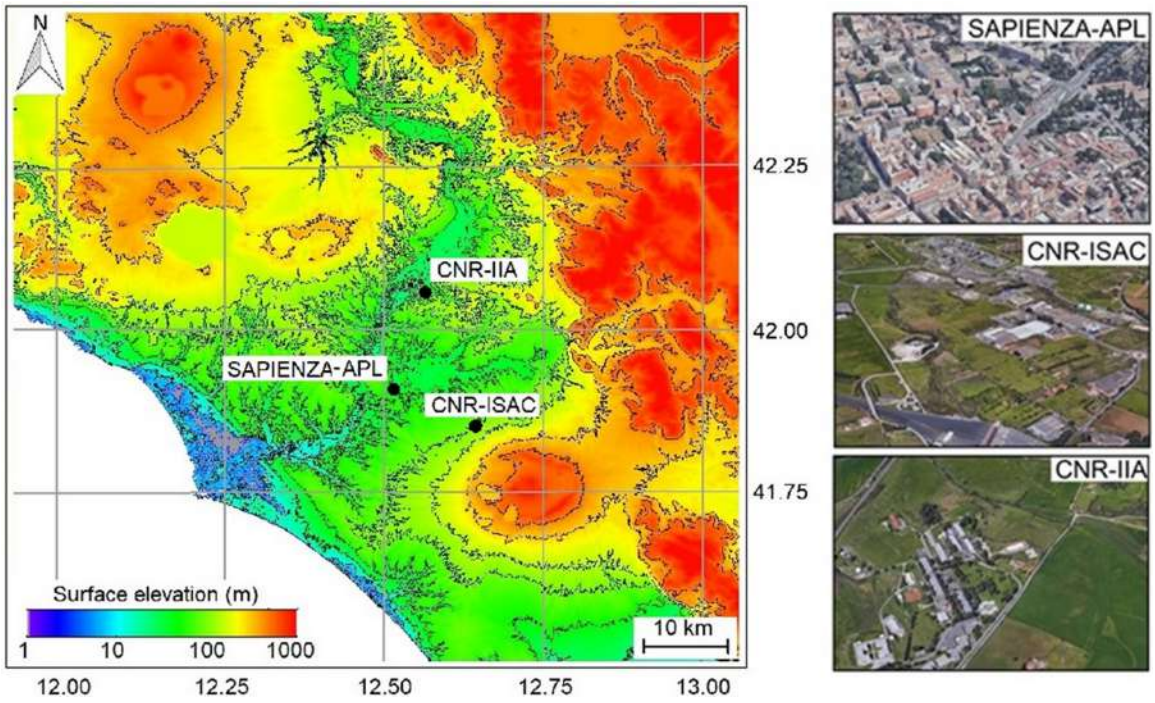

Fig. 1. BAQUNIN sites locations: urban (Sapienza-APL), semirural (CNR-ISAC), and rural (CNR-IIA). Colors depict the Shuttle Radar Topography Mission (STRM) digital elevation model in log scale. The black lines represent the 100-m evenly spaced contour lines.

population living in the urban center, commuters from rural and semirural surroundings reach their workplaces in Rome every day, increasing the traffic volumes on the main business streets, especially during the morning and the late afternoon rush hours.

The region is often exposed to extreme aerosol events, as Saharan dust is frequently transported at these latitudes over the Mediterranean Sea (Gobbi et al. 2013). The supersite has the nontrivial advantage of being located close to Pratica di Mare, one of the major permanent radiosounding stations in Italy run by Italian Air Force, where balloon soundings are regularly performed at 0000 and 1200 UTC. In the BAQUNIN framework, these extremely valuable atmospheric data are used for intercomparison/calibration purposes (e.g., lidar retrievals), for assessing the quality of Weather Research and Forecasting (WRF) Model forecasts by comparing collocated temperature and humidity profiles, for the accurate estimate of tropopause, and for the assessment of atmospheric stability conditions. Hence, the conformation of the city, its geographical position, and its anemological peculiarities make it the convenient site for studies focused on (i) monitoring atmospheric pollution and atmospheric constituents, (ii) providing a UBL characterization, and (iii) providing reference products for satellite and models validation in an urban context. The importance of conducting studies in this region was also recognized by the European Space Agency (ESA), which constantly supported the BAQUNIN project from its very birth, as explained in what follows.

Partners and observation sites. Since 2013 (Casadio et al. 2013), ESA has promoted the creation of an experimental research infrastructure for the validation of present and future satellite atmospheric composition products through a series of initiatives, run under the responsibility of the European Space Research Institute (ESRIN)–Sensor Performance, Products and Algorithms (SPPA) section. In the framework of the "fiducial reference measurement" (FRM) series, several projects dedicated to the improvement of the quality of the ground-based remote sensing instruments are currently active, aiming to provide the community of researchers involved in the satellite calibration and validation (hereinafter cal/val) with elevated standard validation products (https://earth.esa.int/web/sppa/home).

In the context of SPPA, the BAQUNIN precursor activities (small and short-term projects focused on specific scientific and technical topics) started in 2015 in the framework of the Instrument Data quality Evaluation and Analysis Service (IDEAS+) contract (service acting on behalf of ESRIN-SPPA section for ensuring the best data quality of ESA operational Earth observations missions), and continued with the BAQUNIN project from March 2019 onward, to create an atmospheric composition cal/val supersite, allowing for UBL studies and innovative monitoring of the urban environment.

The BAQUNIN consortium is composed of the following entities: (i) Serco Italia (www.serco.com/eu), a private company based in Frascati (Rome, Italy); (ii) the Atmospheric Physics Laboratory (Sapienza-APL), belonging to the Physics Department of the Sapienza University of Rome; (iii) the National Research Council (CNR) Institute of Atmospheric Sciences and Climate (CNR-ISAC), located in the Research Area of Tor Vergata, Rome; (iv) the CNR Institute of Atmospheric Pollution Research (CNR-IIA), located in the Research Area of Montelibretti, Rome.

In its current configuration, the BAQUNIN supersite consists of three observation sites, located at Sapienza-APL [hereinafter APL, latitude 41.90°N, longitude 12.52°E, 75 m above mean sea level (MSL)], CNR-ISAC (hereinafter ISAC, latitude 41.84°N, longitude 12.65°E, 117 m MSL) and CNR-IIA (hereinafter IIA, latitude 42.11°N, longitude 12.64°E, 92 m MSL), i.e., in the Tiber valley surrounding Rome (Fig. 1).

The three sites have been selected in the urban, semirural, and rural environments, to allow in-depth studies of UHI and UPI under different atmospheric characteristics and to support cal/val activity of satellite products. APL is in the Rome city center and hosts the instruments on the rooftop of a six-floor building, at approximately 25 m above ground level (AGL). The ISAC site is located in a flat, semirural environment, about 13 km southeast of Rome, close to the Alban hills. ISAC hosts the CNR-ISAC Rome Atmospheric Observatory (CIRAS; www.isac.cnr.it/en/infrastructures/ciras). The BAQUNIN additional instrumentation reinforces the already existing observatory for meteorological and atmospheric composition studies. The IIA is in the Tiber valley and is considered as a reference for the investigation of rural background atmospheric conditions (it is located about 26 km northeast of Rome). The institute houses the Liberti station (https://en.iia.cnr.it/osservatorio-arnaldo-liberti/), where several instruments routinely carry out chemical aerosol and gaseous compound measurements, also hosting the BAQUNIN facilities.

Meteorological and air quality characteristics of the BAQUNIN sites. The peculiarities of the three sites are highlighted by analyzing the seasonal variability of relevant meteorological parameters, and the concentrations of nitrogen dioxide (NO_2) and ozone (O_3), two pollutants that are commonly monitored and are subjected to regulations.

The year 2019, i.e., the first year of full activity of BAQUNIN, is studied. In addition to the BAQUNIN data, the measurements acquired from nearby stations managed by other agencies or research institutions were also considered. Specifically, meteorological data for ISAC and in situ O_3 concentration for APL are provided by the Regional Environmental Protection Agency of Lazio region (ARPA Lazio) air quality network, while meteorological data and in situ concentrations of NO_2 and O_3 for IIA are furnished by the Liberti station.

Figure 2 shows the seasonal wind roses, obtained following the astronomical season's classification, and the differences in the anemological conditions at the sites. At APL, the sea–land-breeze regime is predominant in summer, when the wind essentially blows from the southwest quadrant and from northeast. In the remaining seasons, the wind chiefly blows from north-northeast and from south-southeast, with higher intensities in the latter case. The wind roses relative to ISAC depict a rather homogeneous distribution of wind directions and intensities, essentially due to the orography of the area: the proximity of the hills on one side and the Tiber valley on the other complicate the local circulation pattern, impairing the predominance of a definite direction. Nevertheless, the contribution of the breeze regime is

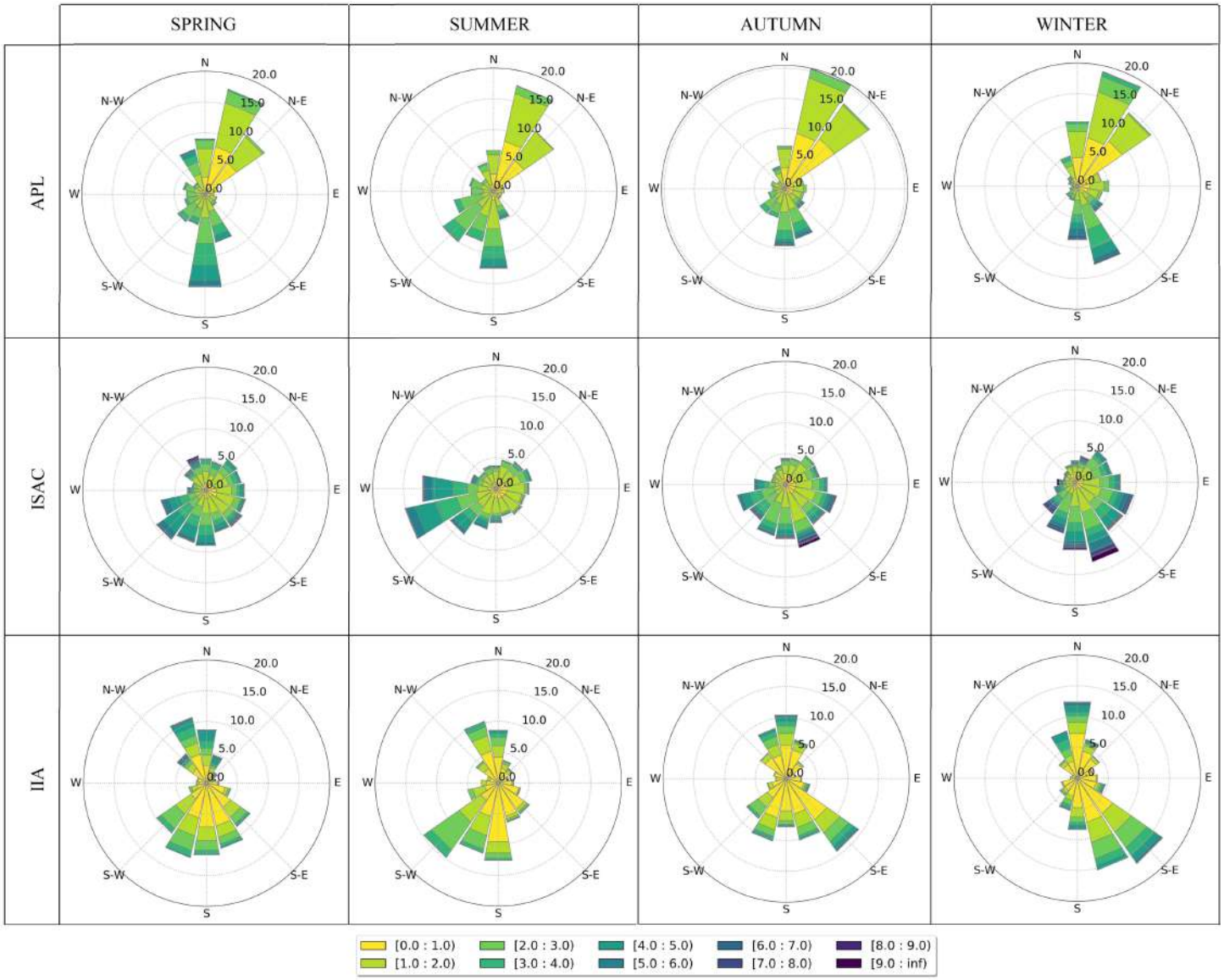

Fig. 2. Seasonal wind roses for 2019 computed for (top) APL, (middle) ISAC, and (bottom) IIA for (left to right) spring, summer, autumn, and winter, respectively. The colors depict the horizontal wind intensity (m s^{-1}).

evident in summer, with prevailing and dominant winds from the west-southwest direction. The winds at the IIA site are also closely linked to the orography of the region, the prevailing directions being from the north and south quadrants, i.e., coinciding with the direction of the valley axis, throughout the year. It should be noted that the APL meteorological station is installed 28 m AGL (on the edge of the rooftop of a building about 25 m high), while ISAC and IIA stations are 10 and 4 m AGL, respectively.

Figure 3 shows the weekly averages of air temperature (T), absolute humidity (AH) computed following Camuffo (2010), and total precipitation (TP) for the three sites, measured by surface weather stations. The regimes of the average daily temperatures (Fig. 3a) are very similar, although APL always shows slightly higher values than the other sites (about 0.9°C more than ISAC and 1.6°C more than IIA). The minimum values are also higher in the urban environment than at the other two sites (about 2°C during the summer), while maxima are 1°C higher at IIA with respect to APL and ISAC. These temperature differences depend on the different height above sea level and distance from the coast across the stations. Moreover, the different land surface characteristics give rise to the UHI phenomenon in the center of Rome, which induces an increase in temperatures in the urban area, especially during summer and

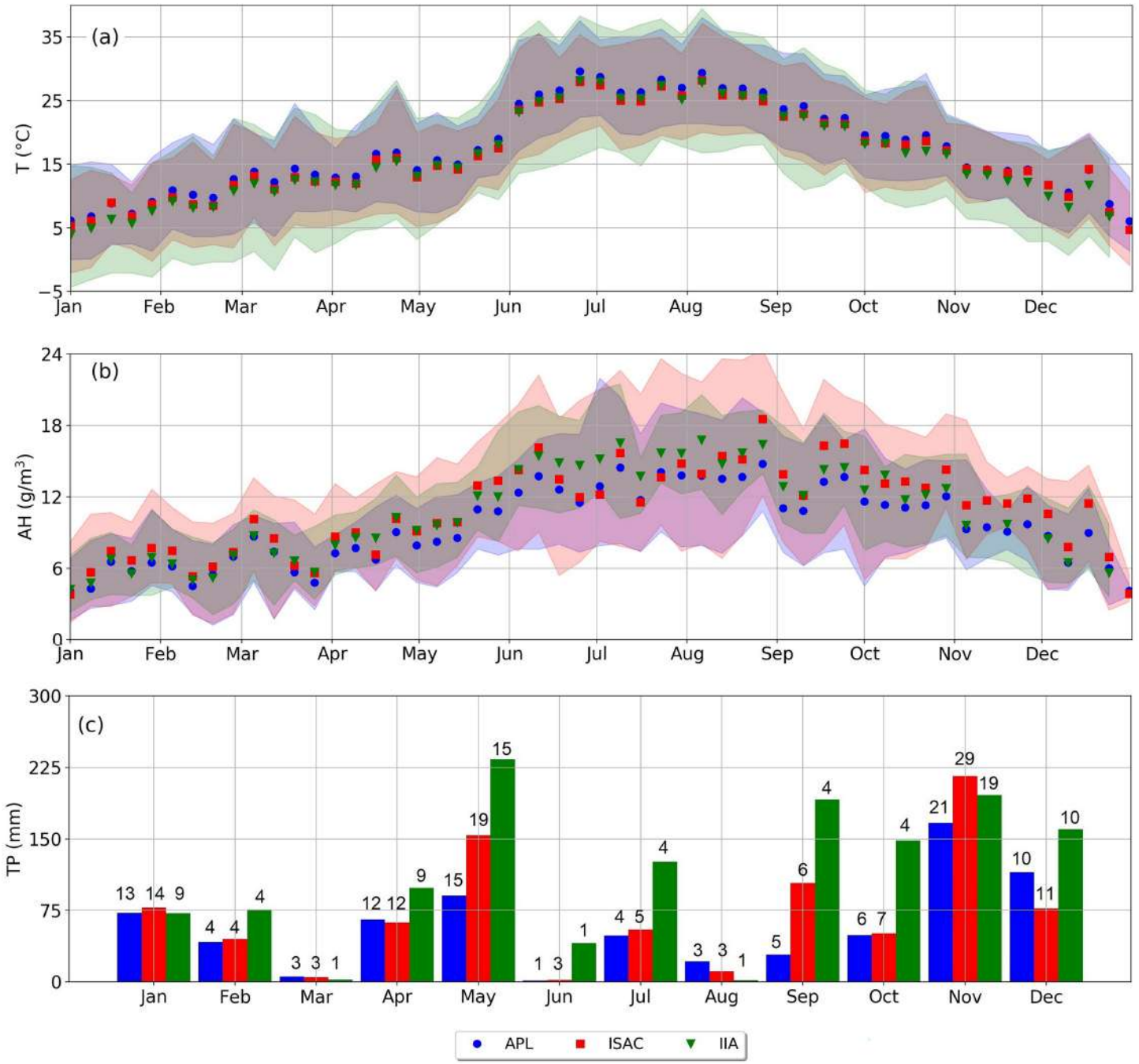

Fig. 3. Weekly temporal variations of (a) air temperature (*T*), (b) absolute humidity (AH), and (c) total precipitations (TP) for the year 2019 for APL (blue dots), ISAC (red squares), and IIA (green triangles). The shaded areas in (a) and (b) show the daily minimum and maximum values of *T* and AH; numbers in (c) depict the number of rainy days.

at night, as pointed out, for instance, by Ciardini et al. (2019). APL is the warmest site: the highest minimum temperatures are usually recorded (due to the UHI effect), also resulting in the highest average temperatures. The AH weekly median values (Fig. 3b) at APL range between 4.1 and 14.8 g m^{-3} (annual median: 9.3 g m^{-3}), while ISAC generally exhibits the highest absolute humidity (annual median: 11.4 g m^{-3}), except in summer, when AH locally experiences a significant drop coherently with the seasonal variations in total precipitation and in the number of rainy days (Fig. 3c). In fact, during June and July, IIA is characterized by precipitation amounts that are much higher (about 300% more) than at the other sites, also responsible for the highest AH values.

Figure 4 shows the weekly average surface concentrations of NO_2 (Fig. 4a) and O_3 (Fig. 4b) available for APL and IIA only. Urban NO_2 concentrations fluctuate between 15 and 60 ppb,

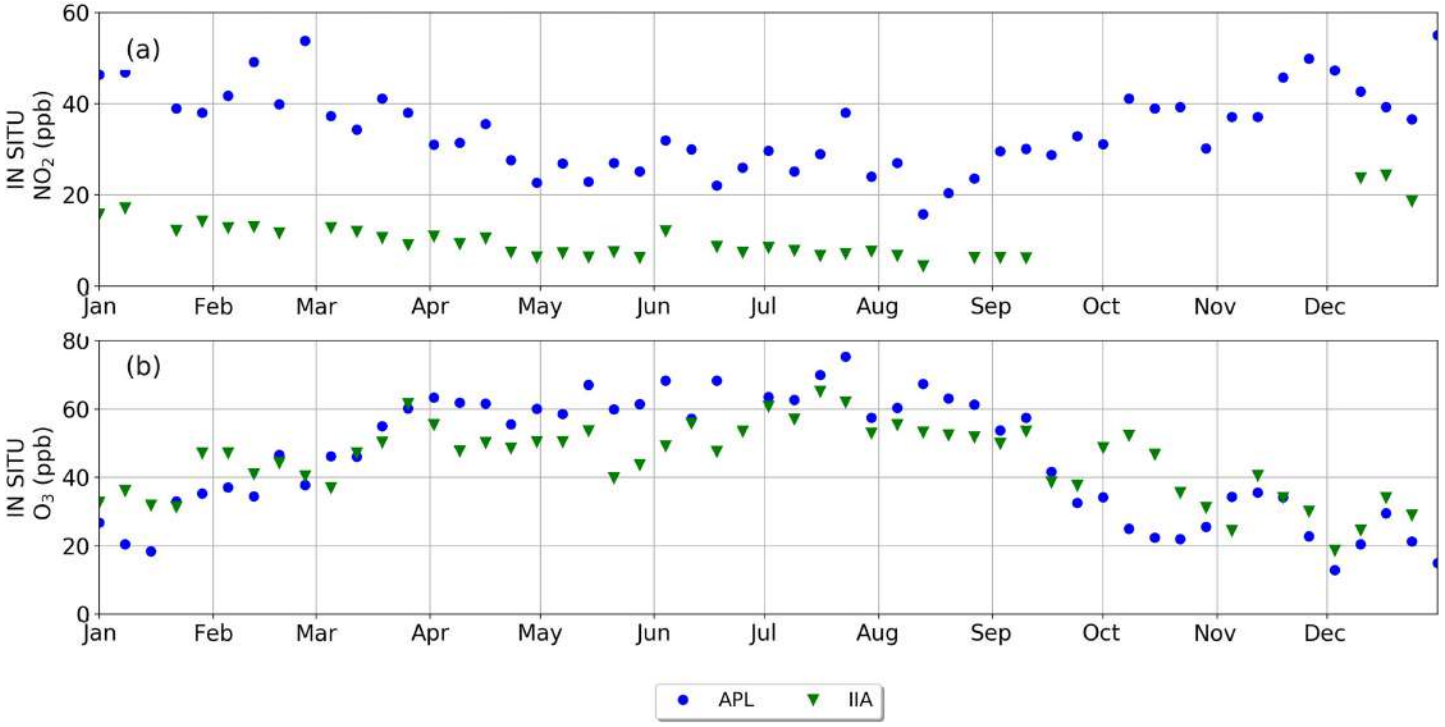

Fig. 4. Weekly temporal variations of in situ concentrations of (a) NO_2 and (b) O_3 for the year 2019 for APL (blue dots) and IIA (green triangles).

while they are much lower in the rural area, with average values of about 7 ppb and peaks of 25 ppb. In both sites, the concentrations are lower in summer (about 45 ppb at APL and 8 ppb at IIA), due to the shorter lifetime and to the weaker anthropogenic local sources typical of the summer months. The in situ O_3 shows values typically between 10 and 75 ppb, with a marked and similar seasonal cycle in IIA and APL, assuming higher values in summer (about 60 ppb at APL and 55 ppb at IIA) than in winter (about 20 ppb at APL and IIA).

Main knowledge gaps and research challenges

In Rome, during the past two decades, a significant number of scientific campaigns were carried out. For instance, Struckmeier et al. (2016), characterized the urban aerosols in Rome downtown, studying their seasonal and spatial variability, dynamics, and main sources, Mallone et al. (2011) investigated the effect of Saharan dust on the association between different PM fractions and daily mortality in Rome. Recently, Ciardini et al. (2019) used micrometeorological in situ measurements to evaluate the distribution of the UHI intensity in and around the city, while Pelliccioni et al. (2020) focused on the role played by micrometeorology and indoor airflow characteristics in determining indoor PM concentration. Nonetheless, these were short, intensive campaigns, which did not provide information about the long-term evolution of the urban atmospheric characteristics.

In general, despite the presence of instruments dedicated to the meteorological characterization and the investigation of specific phenomena, often past research projects provided data that did not allow an accurate and comprehensive atmospheric analysis, also due to the scarcity of continuous profile measurements. The latter, in synergy with columnar and ground-based observations would definitely improve the knowledge of the urban atmosphere and provide a complete dataset for the accurate validation of satellite products.

Due to the exiguity of long-term measurements, which can provide information on current trends, near-future scenarios of the urban atmosphere evolution are obtained through simulations (Chen et al. 2011). Numerical results, however, are affected by considerable uncertainties as they require, for the determination of boundary conditions and for the validation of results,

the knowledge of source emission and land use, i.e., environmental characteristics continuously changing and hard to assess (Nahian et al. 2020). High-quality measurements, such as those provided by BAQUNIN, can effectively be used to validate and calibrate numerical projections, by providing realistic profiles in the UBL (e.g., of wind speed and direction and of turbulent kinetic energy) and thermal fluxes.

As a matter of fact, current atmospheric composition products from space cannot be used for accurate UBL studies (Huang et al. 2021). Limiting factors are the still too low spatial resolution [3.5×5.5 km^2 for nadir observations of the Tropospheric Monitoring Instrument (TROPOMI), a sensor on board the Copernicus *Sentinel-5 Precursor* (*Sentinel-5P*) satellite], and the low sensitivity of the measured radiance to the lowest portion of the atmosphere. Additionally, due to the spectral and spatial inhomogeneity of the surface affecting ground reflectivity and to the sharp horizontal variation of the atmospheric conditions, observations from satellite-borne sensors cannot correctly capture differences in the atmospheric structure between surfaces with different dynamical and thermal features. Other limitations are (i) the low temporal resolution [for low-Earth-orbit (LEO) satellites], which does not fully capture the daily cycles of pollutant concentrations (e.g., photochemistry) and (ii) the significant uncertainties in the airmass factor, due to aerosol scattering and to insufficient information on species profiles close to the surface and on the height of the UBL.

Despite all the efforts made so far, the necessity of acquiring high-quality and long-term atmospheric measurements in the urban environment is therefore evident. In this context, BAQUNIN can provide a valuable contribution to bridging these knowledge gaps, providing synergistic information on meteorological parameters, columnar content of trace gases and aerosol, vertical stratification of particulate matter, and solar irradiance, allowing the detailed study of the UHI, of the UPI, and of the interaction between the local and the mesoscale circulation and pollution. These data, while enriching preexisting databases, also play a key role in the validation of the latest generation satellite products, as BAQUNIN produces and distributes free data for satellite validation activities through international networks and portals. These products are also useful to the scientific community, allowing for intercomparison exercises and for intercalibration campaigns of ground-based instruments that are routinely used for cal/val activities.

In recognition for the potentialities of the BAQUNIN products in the satellite cal/val context, the NO_2 total columns from BAQUNIN instruments are routinely used by the *Sentinel-5P* Mission Performance Center (https://mpc-vdaf-server.tropomi.eu/) for the validation of TROPOMI Real-Time and Offline products (see, e.g., Verhoelst et al. 2021). The BAQUNIN team is also currently involved in two ESA Announcement of Opportunity cal/val projects, namely, the "EarthCARE" and "Copernicus *Sentinel-5P* TROPOMI" validation projects. For the EarthCARE mission (Illingworth et al. 2015), the comparison between observations and satellite data will contribute to the improvement of the inversion algorithms, by validating a set of aerosols and cloud-related products collected in sites that are representative of different scenarios. As to the TROPOMI mission (Veefkind et al. 2012), BAQUNIN provides data for the direct validation of O_3, NO_2, water vapor, formaldehyde, sulfur dioxide, tropospheric vertical column, thus evaluating the impact of different aerosol types and loads. The BAQUNIN Satellite cal/val activities include the validation of Sentinel-3 aerosol optical depth (AOD) products, and the so-called ESA third party missions (TPMs), such as the Global Change Observation Mission–Climate Second Generation Global Imager (GCOM-C SGLI) (Tanaka et al. 2018) and the Thermal And Near-infrared Sensor for carbon Observation–Fourier Transform Spectrometer (TANSO-FTS) on board the *Greenhouse gas Observation Satellite* (*GOSAT*) (Suto et al. 2021).

The CNR, the Italian National Agency for New Technologies, Energy and Sustainable Economic Development (ENEA), the National Institute of Geophysics and Volcanology (INGV), Serco, Sardegna Clima Onlus, and Sapienza University all actively participate in the cal/val activities. The validation activities for TPMs, in particular, are carried out also in close collaboration with the ESA Earthnet Data Assessment Project (EDAP; https://earth.esa.int/eogateway/activities/edap).

Equipment and products

BAQUNIN includes active and passive remote sensing and surface instruments, which allow the retrieval of fundamental parameters for the investigation of atmospheric properties, gases, and atmospheric aerosols. Most of the devices currently installed in APL are purchased (see Table 1 for details), except for the APL multiwavelength (MWL) light detection and ranging (lidar) and the sound detection and ranging (sodar), which are custom-made. A dual spectrometer system Pandora-2S is installed at both ISAC and IIA sites. In support to the observational activities, the BAQUNIN consortium produces dedicated numerical simulations of the relevant meteorological fields by means of the WRF Model (Skamarock et al. 2008).

The advantageous location of its three stations, and the contemporary presence of several diverse instruments for atmospheric observation, have fostered the insertion of BAQUNIN in several national and international remote sensing networks, for which it now represents a certified cross-point. These networks are

Table 1. Brief description of the commercial instruments belonging to BAQUNIN observatory, the manufactory, the network's web addresses, and the sites where they are currently installed.

Instrument description	Site
Ceilometer Raymetrics Aerosol Profiler (RAP): Automated eye-safe infrared elastic lidar. Emitting source: a diode-pumped Nd: YAG laser with wavelength 1,064 nm, pulse energy 30 μJ, and repetition rate 5 kHz. Receiver: Cassegrain telescope, diameter 200 mm and Avalanche Photodiode (APD) detector. Full overlap range altitude: 250 m; vertical range resolution: 7.5 m; raw signal range: 14 km. Raymetrics, Athens, Greece: https://raymetrics.com/	APL
Prede-POM radiometer: Narrowband filter photometer performing measurements of direct solar and diffuse sky irradiances at several scattering angles in the almucantar and principal plane geometries, at selected wavelengths in the range 315–2,200 nm. Prede Co. Ltd., Tokyo, Japan: www.prede.com/english/index.htm Network: www.euroskyrad.net/	APL
Cimel-CE318: Photometer performing direct solar irradiance and sky (radiance) observations for selected wavelengths between 340 and 1,640 nm. Cimel Electronique, Paris, France: www.cimel.fr/ Network: https://aeronet.gsfc.nasa.gov/	APL
Pandora-2S: Dual spectrometer system taking measurements in the spectral range 290–900 nm using two spectrometers with a resolution of 0.6 nm. The system can perform direct sun, zenith sky, principal plane, or almucantar observations with a 0.01° pointing precision. SciGlob Instruments and Services, Elkridge, United States: www.sciglob.com/ Network: www.pandonia-global-network.org/	APL ISAC IIA
Brewer MKIV: Single-monochromator spectrophotometer to measure global spectral UV irradiance (range 290–325 nm at 0.5-nm step), and to retrieve, from direct-sun and zenith-sky solar radiation, O_3, and sulfur dioxide (at specific wavelengths in the UV between 310 and 320 nm), and NO_2 (at specific wavelengths in the visible range between 425 and 453 nm). Kipp and Zonen, Delft, the Netherlands: http://kippzonen-brewer.com/ Network: www. rbcce.aemet.es/eubrewnet org, www.woudc.org	APL
Pyranometer, Hukseflux SR11: High-accuracy actinometer measuring solar radiation in the 285–3,000-nm spectral range. Hukseflux Thermal Sensor Company, Delft, the Netherlands: www.hukseflux.com/	APL
Meteorological station OMD, Vaisala, WXT520: The station provides measurements of relative humidity, temperature, wind speed, and wind direction. Vaisala, Helsinki, Finland: www.vaisala.com/en Network: www.fondazioneomd.it/	APL
Meteorological station SCO, Davis Vue 6357: The station provides measurements of temperature, rain, dewpoint, pressure, wind speed, wind direction, and UV index. Davis Instruments Corporation, Hayward, United States: www.davisinstruments.com/ Network: www.sardegna-clima.it/	APL
Microbarometer, Vaisala PTB200A: Fully compensated digital barometer designed to operate over a wide pressure and temperature range. Resolution: 0.01 hPa. Vaisala	APL

- Pandonia Global Network (PGN; www.pandonia-global-network.org): the network of Pandora instruments, promoted by ESA and by the National Aeronautics and Space Administration (NASA);
- SKYNET/European Skynet Radiometers (ESR; www.euroskyrad.net/): the European branch of the Skynet radiometers network of Prede-POM sun sky radiometers;
- Aerosol Robotic Network (AERONET; https://aeronet.gsfc.nasa.gov/): run by NASA and Laboratoire d'Optique Atmosphérique (LOA-PHOTONS) (www-loa.univ-lille1.fr/photons);
- European Brewer Network (EUBREWNET) (www.eubrewnet.org/): the network of European Brewer Spectrophotometer monitoring stations launched as part of a COST Action;
- Climate Network (OMD; https://fondazioneomd.it/climate-network): Italian national network of certified quality weather stations;
- Sardegna Clima (SCO; www.sardegna-clima.it/): Sardinian network of weather stations.

The BAQUNIN instruments that are included in such officially recognized networks are subject to quality control, thus assuring community-certified quality data (for each network, more details on the specific best practice procedures and protocols are available on the websites aforementioned). For those instruments that do not belong to a network, specific procedures are anyway followed to verify the quality of measurements and retrievals, according to the guidelines provided by the manufacturers or by the scientific community (for each product, see the references in Table 2). Finally, for the custom-made instruments, statistical analyzes are carried out and, for the MLW lidar, the guidelines provided by Aerosols, Clouds, and Trace gases Research Infrastructure (ACTRIS) and the European Aerosol Research Lidar Network

Table 2. List of products supplied by BAQUNIN.

Product	Instrument	References	Data availability
Gases			
O_3 TC	Brewer	Siani et al. (2018)	1992–today
NO_2 surf, NO_2 trop	Pandora-2S	Herman et al. (2015)	2016–today
NO_2 TC	Brewer	Diémoz et al. (2021)	1996–2017
H_2O TC	Cimel-CE318	Berezin et al. (2017)	2017–today
Aerosol			
AOD, AE	Cimel-CE318	Giles et al. (2019)	2017–today
	Prede-POM	Nakajima et al. (2020)	2010–today
	Lidar (MWL and RAP)	Klett (1985)	2016–today
AerBack, AerExt profiles	Lidar	Klett (1985)	2016–today
SAE, AAE	Cimel-CE318	Klett (1985)	2017–today
SSA, VSD, refr. index, PF	Cimel-CE318	Giles et al. (2019)	2017–today
	Prede-POM	Kudo et al. (2021)	2010–today
Meteo			
H	Pyranometer	Azouzoute et al. (2019)	2018–today
UVI, UVD	Brewer meteorological station SCO	Fountoulakis et al. (2021)	1996–today
Profiles of U and θ	Sodar	Mastrantonio and Fiocco (1982)	2007–10, 2017–today
Surface measurements: U, θ, T, RH	Meteorological station SCO and OMD	—	2019–today
P	Microbarometer	www.vaisala.com/sites/default/files/documents/PTB200_User_Guide_in_English.pdf	2020–today
RI, DP	Meteorological station SCO	—	2020–today

(EARLINET) are followed. In addition, daily checks are performed to ensure the continuity of the acquisition and avoid gaps in the datasets.

MWL lidar description. The MWL lidar has been designed and assembled using both custom-made and commercial equipment. The laser source, sensors, electronics, and optics are components commonly available from serial industrial production, while frames and optomechanics were designed and built by the APL/BAQUNIN team. The controlling software has also been developed in-house. This modular approach allows a regular upgrading of single components and permits to add new acquisition channels to the basic instrument to improve the system performance.

Presently, the system includes a powerful-pulsed laser, four optical receivers (telescopes), and 12 acquisition channels. The Quanta Ray Pro-290-30 laser produces 10-ns pulses at three wavelengths, 1,064, 532, and 355 nm, with nominal pulse energy of 1,600, 800, and 400 mJ, respectively. The three beams are injected into the atmosphere by adjustable mirrors and prisms. The MWL lidar backscattered signals are collected by four receivers and the acquisition system is based on six transient recorders TR20 at Licel equipped with an analog-to-digital converter (ADC) as well as with a photon counter. The system's maximum range is 22.5 km, although the signal-to-noise ratio reduces the retrieval capability above the tropopause. In what follows, the information about the minimum and full overlap altitudes refer to the current configuration, albeit the alignment of the receivers is adjustable for specific studies concerning the PBL. The receiver for ultraviolet (UV) high range is a 50-cm Cassegrain telescope (minimum and full overlap altitudes: 300 and 5,000 m MSL, respectively) for elastic backscattering at 355 nm, molecular nitrogen (N_2) at 386 nm, and water vapor at 407 nm for Raman backscattering. Three photon-counting channels are used for these signals and an additional analog channel is dedicated to the Raman water vapor signal.

Two telescopes are devoted to the visible (VIS) elastic backscattering at 532 nm: the low-range receiver is a 6-cm refractive telescope (minimum and full overlap altitudes: 120 and 150 m MSL, respectively), while the high range is a 10-cm Cassegrain telescope (minimum and full overlap altitudes: 200 and 500 m MSL, respectively). Low- and high-range 532-nm backscatter signals are merged following the Licel procedures (Mielke 2005). Four analog channels are dedicated to total and parallel polarization of 532-nm elastic signals. Finally, the infrared (IR) receiver is a 10-cm Cassegrain telescope (minimum and full overlap altitudes: 250 and 400 m MSL, respectively) used for the total elastic backscattering at 1,064 nm, acquired by an analog TR20 channel. The TR20 device permits a vertical resolution of 7.5 m and a user-defined time resolution of 10 s. The delay between the laser pulse emission and the zero bin of the profile recorded by every TR20 has been measured following the procedure suggested in Freudenthaler et al. (2018) and corrected during the inversion procedure.

Lidar measurements are collected in connection to overpasses of selected satellites within 150 km from the APL location. Further measurement sessions can be scheduled based on calibration/scientific needs. Typically, acquisitions start in the morning until mid–late afternoon.

The basic inversion procedure for inferring the vertical profile of aerosol volume backscatter and extinction coefficient at 355, 532, and 1,064 nm is the Klett-modified iterative procedure, assuming an extinction-to-backscattering ratio [lidar ratio (LR)] that is constant with altitude (Di Girolamo et al. 1999). The molecular signal needed in the retrieval process is calculated from temperature and pressure profiles measured by radiosondes launched at Pratica di Mare (latitude 41.65°N, longitude 12.43°E, about 25 km south of APL). Note that Pratica di Mare is a coastal site while APL is fully embedded in the urban canopy of the city of Rome. This implies that radiosounding information on boundary layer cannot be directly used in synergy with BAQUNIN data. However, the free-tropospheric portion of the radiosonde profiles are routinely used for the calibration of the MLW-lidar aerosol products. The 355-nm signal

retrieval employs the ratio between UV and N_2 Raman profiles, to extract information below the total overlap altitude as in Ansmann et al. (1992). The LR value is imposed according to the predominant aerosol type inferred by the back-trajectory study from literature. Cattrall et al. (2005) suggested values for 1,064 nm (37 ± 6 sr and 35 ± 5 sr for urban and dust), and 532 nm (71 ± 10 sr and 42 ± 4 sr for urban and dust), while Müller et al. (2007) proposed 58 ± 12 sr for urban aerosols and 55 ± 6 sr for dust at 355 nm. In fair weather, the BAQUNIN's photometers (Cimel-CE318 and Prede-POM) provide independent measurements of aerosol LR at different wavelengths. When available, these values are used in the inversion process, together with their associated uncertainty, to better estimate backscatter and extinction coefficient profiles. The lidar signal depolarization is a useful tool for the study of the thermodynamic phase of aerosol and cloud particles. In the MWL lidar, the retrieval of the aerosol volume depolarization ratio is obtained using the 532-nm total and parallel-polarized signal at short and far range. The equipment for automatic calibration using the 45° method, described in Freudenthaler et al. (2018), is installed only on the 532-nm high-range receiver. The duplication and installation of the same apparatus on the low-range receiver is planned. When signal noise is low enough, the extinction coefficient and LR can be calculated using the Raman N_2 signal as in Ansmann et al. (1992).

Sodar description. The APL three-axis Doppler sodar has been operational since 1990. Currently, the instrument is in monostatic configuration with a pulse repetition rate of 3 s. The three antennas simultaneously emit 0.1-s-long acoustic bursts at the sound frequencies of 2,750, 3,000, and 3,250 Hz. Two of them are 20° tilted from the zenith, while the third is aligned vertically. The pointing azimuth angles for the two tilted antennas are 60° and 330° with respect to north. In this configuration, the overlap of the three antenna beams is avoided and the instrument can provide the vertical profile of both the atmospheric thermal turbulence and the horizontal wind speed and direction (along with the vertical wind speed and its standard deviation) up to a maximum probing altitude of 518 m MSL with a vertical resolution of 4.5 and 18.2 m, respectively. Wind velocities are obtained via a Doppler analysis following the two-step procedure described in Mastrantonio and Fiocco (1982), which permits to determine the three-antenna radial velocities with a precision of 0.1 m s^{-1}. More details about the description of APL sodar electronic components and signal processing techniques can be found in Mastrantonio et al. (1994). The echo intensity measured by the vertical antenna provides a picture of the atmospheric structure, including peculiar features such as thermal plumes, nocturnal inversions, waves, and fronts. During the past two decades, the APL sodar has been used to characterize the UBL (Rao et al. 2004), also in synergy with other remote sensing devices (Rao et al. 2002) and with mesoscale numerical simulations (Pichelli et al. 2014).

WRF setup description. The BAQUNIN measurements are accompanied and supported by numerical forecasts of the relevant meteorological fields, obtained by running the WRF Model (WRF-ARW, version 3.9.1). The model domain includes Rome, the Tiber's valley, and its suburban areas in central Italy (central latitude: 42.20°N; central longitude: 12.75°E). It uses a three two-way nested domains configuration, with grid resolution ranging from 9 to 3 to 1 km, corresponding to 108 × 108, 106 × 106, and 106 × 106 grid points, respectively. Forty unevenly spaced vertical levels (from ~30 to 21,000 m) are used for all domains, up to a maximum height of 50 hPa. Vertical resolution is highest in the lower atmosphere.

As a baseline, the time resolution of WRF output is 15 min, with the possibility to increase/decrease it depending on the application needs. The WRF output include 36 h of forecast. The simulations start automatically at 0400 UTC of the current day using the 0000 UTC 0.25° Global Forecast System (GFS) forecast, provided by the National Centers for Environmental

Prediction (NCEP) at National Oceanic and Atmospheric Administration (NOAA), from 0 to +36 h as the initial and boundary conditions The downscaled WRF forecasts are used to investigate the role of advection/transport of aerosols and trace gases in the BAQUNIN research area. The extraction of relevant parameter profiles and surface values for the APL, ISAC, and IIA sites (e.g., wind, temperature, and humidity) is also performed automatically as soon as the forecasts are produced and promptly made available to the community via web services. The calculation of forward/backward trajectories is performed for the BAQUNIN sites for specific cases, e.g., during the unfortunately frequent occurrence of wild or industrial fires in the proximity of Rome.

Products and dissemination. Table 2 summarizes the atmospheric products retrieved in the framework of BAQUNIN activities. For each variable, the measuring instrument, the references for the retrieval algorithm, the accuracy (when available), and the data availability are provided. Updates of the product list, as well as additional information about the instruments, can be found on the BAQUNIN website (www.baqunin.eu).

The retrieved parameters can be grouped into three categories: gas, aerosol, and meteorology. The currently retrieved gases are O_3, NO_2, and water vapor, using different measurement geometry: direct-sun and zenith-sky measurement for total column (TC) amounts, and diffuse radiance sun measurements for surface and tropospheric (surf and trop) amounts. The columnar aerosol parameters are obtained in direct-sun, principal plane, and almucantar geometries. These are AOD, Angstrom exponent (AE), scattering and absorption Angstrom exponent (SAE and AAE), single scattering albedo (SSA), volume size distribution (VSD), real and imaginary part of refractive index (refr. index), and phase function (PF). The aerosol backscattering and extinction (AerBack and AerExt) profiles are also provided. The meteorological parameters, mainly obtained using in situ instruments, are surface and dewpoint air temperature (T, DP), relative humidity (RH), atmospheric pressure (P), rainfall intensity (RI), and wind speed (U) and direction (θ). The vertical profiles of the last two parameters are retrieved using the sodar. Finally, the hemispherical radiance (H) and the ultraviolet spectra are obtained from downward radiation measurements and are used to determine the ultraviolet dose and index (UVD and UVI, respectively).

Because the BAQUNIN suite of products is produced by a variety of instruments and processing chains, some differences in the native data formats, naming conventions, and physical units of the observed parameters may occur. Thus, a substantial effort is put into the harmonization of all BAQUNIN data, converting all native datasets into netCDF file format, and, when applicable and feasible, following the GEOMS standards for atmospheric products for the formatted metadata.

The BAQUNIN data are collected in centralized storage located at APL. The hardware infrastructure consists of storage arrays configured to ensure both dynamic data redundancy and data interactive access. The stored files include the raw files that are saved by the acquisition software, all ancillary files required for the processing chain and the monitoring of the instruments during the acquisition, and the files created in the subsequent phases of data analysis.

The final products are disseminated through three main platforms available to the users: (i) international networks, in the native formats; (ii) BAQUNIN website, in netCDF format (www.baqunin.eu); and (iii) ESA Atmospheric Validation Data Center (EVDC; https://evdc.esa.int), in the GEOMS formats. EVDC is a central, long-term repository in Europe for archiving and exchange of correlative data for validation of atmospheric composition products from satellite platforms.

As the BAQUNIN products also provide useful information for improving the quality of everyday life, the dissemination of products not only reaches the scientific community, but also the general public. In fact, BAQUNIN produces useful information for both policy-makers and the population, communicating in a simple and immediate way to citizens the state of air pollution in several areas, so that they are aware of the air quality they are breathing, in

terms of presence of gaseous contaminants and aerosols, also providing information on past, present, and near-future weather conditions.

Furthermore, BAQUNIN activities can significantly contribute to the third mission of the University of Rome (www.uniroma1.it/it/pagina/terza-missione), i.e., seeking to generate knowledge outside academic environments to the benefit of social, cultural, and economic development.

BAQUNIN research lines

The main research activities currently carried out at BAQUNIN are

- the physical interpretation of data collected by numerous remote sensing instruments, operating in synergy, to obtain information about air quality (e.g., aerosol, NO_2, O_3, sulfur dioxide, formaldehyde, and water vapor);
- the investigation of meteorological processes occurring in the PBL, in terms of surface meteorological parameters, low-level wind, and turbulence intensity, daily evolution of the PBL structure, hemispherical solar radiation, and tropospheric clouds observation;
- micro- and local-scale analyses of atmospheric dynamic phenomena, such as sea–land-breeze regime, UHI, and severe events with the comparison between urban and non-urban conditions;
- the study of the effects of medium- and long-range aerosol transport on the atmospheric composition and the physical/optical aerosols properties;
- the design and development of lidar systems and algorithms for the investigation of aerosols and water vapor;
- algorithms development for retrieval of additional products not foreseen by the software supplied with the instruments;
- serving as an intercomparison site for remote sensing instruments belonging to national and international networks; and
- satellite cal/val activities in urban, semirural, and rural environments.

In addition to the above research activities, the BAQUNIN consortium actively participates in the design and organization of measurement campaigns, and is part of several projects, in collaboration with several international and national research institutes, such as

- Effect of Megacities on the Transport and Transformation of Pollutants on the Regional to Global Scales (EMeRGe; www.iup.uni-bremen.de/emerge/home/home.html),
- integrated evaluation of indoor particulate exposure (VIEPI; Pelliccioni et al. 2020),
- Quality and Traceabiliy of Atmospheric aerosol Measurements (QUATRAM; www.euroskyrad.net/quatram.html; Campanelli et al. 2018),
- Metrology for Aerosol Optical Properties (MAPP; www.pmodwrc.ch/en/MAPP/),
- Seagull Borne Atmospheric Measurements (SBAM), and
- Compact Raman lidar for Atmospheric CO_2 and Thermodynamic profiling (CONCERNING).

Finally, BAQUNIN offers hospitality to scientists at its observatory sites, providing an opportunity to place additional instruments managed by other research institutes.

Exploitation of the BAQUNIN products: A practical example

As an example of the BAQUNIN monitoring capability, we show the observations carried out on 11 December 2018, in coincidence with a large fire that broke out overnight at a mechanical–biological waste treatment facility (latitude 41.97°N, longitude 12.51°E, 18 m MSL, hereinafter TMB) managed by the municipal waste management company (Fig. 5a). The fire affected a 2,000-m^2 waste-collection center located in the northern part of

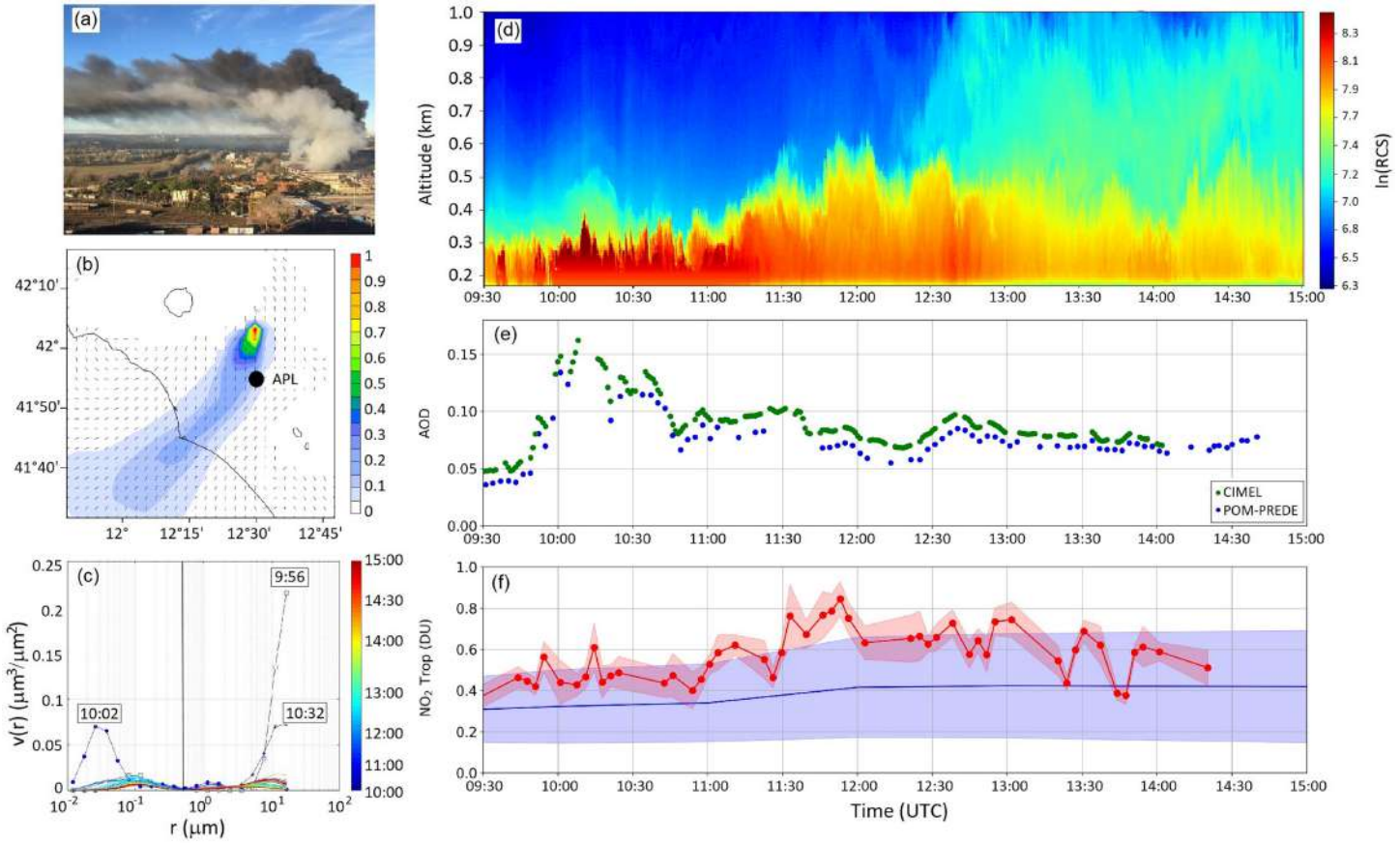

Fig. 5. (a) Plume generated by the fire at the TMB plant on 11 Dec 2018, (b) WRF dimensionless smoke concentration and wind field (150 m MSL) at 1000 UTC, (c) volume size distribution from Prede-POM, (d) logarithm of the range- and overlap-corrected backscatter at 1,064 nm from the lidar, (e) AOD at 500 nm retrieved from Cimel-CE318 (green dots) and Prede-POM (blue dots), (f) NO_2 tropospheric amount (red dotted line) with its standard deviation (red shaded area) compared to the 2016–19 reference period (blue line) with its standard deviation (shaded blue area).

the city, producing thick smoke that could be smelled even in the city center. The city council advised people in the area to keep their windows closed and refrain from outdoor activities. Among the large number of substances released into the atmosphere during the waste combustion, our analysis is focused on the aerosol and NO_2 observed at the APL site. Figure 5b shows the map of dimensionless smoke concentration superimposed to the wind field at 150 m MSL, as obtained by the WRF simulation at 1000 UTC. Starting from the TMB location, the plume produced by the fire appears to be transported toward the city center by the near-surface atmospheric circulation, hitting partially the APL station. In correspondence with the transit of the smoke plume above the city, the values of aerosol size distribution retrieved from Prede-POM observations (Fig. 5c) showed a strong increase of coarse particles (radius greater than 5 μm) at 0956 UTC, probably related to the arrival of ash, followed (1002 UTC) by an increase of the fine mode, associated with the arrival of smaller particles typical of fire plumes, and then presumably by a second peak of ash at 1032 UTC. A sudden increase in the low-altitude aerosol content was detected by the APL MLW lidar from 0945 to 1100 UTC (Fig. 5d). At the same time, the 500-nm AOD measured by Cimel-CE318 and Prede-POM sun photometers increases from 0.02 to more than 0.15 (Fig. 5e).

The evolution of the NO_2 tropospheric columnar content, observed by Pandora-2S on the day of the fire, is shown in Fig. 5f, together with the reference diurnal cycle obtained by the monthly averaged Pandora-2S data during the period 2016–19. The morning increase—larger than one standard deviation with respect to the reference values—suggests that the TMB fire injected a relevant quantity of NO_2 in the troposphere, even if only a negligible amount

reached the surface, since the air quality monitoring network operated by ARPA Lazio in the city center did not detect any anomaly in the concentrations. The measurements carried out by the BAQUNIN suite of instruments therefore appear to be capable of providing useful information to anticipate deposition episodes well before they are detected by surface stations.

Conclusions and perspectives

Thanks to the geographical distribution of its stations and to the wide range of instruments available, the BAQUNIN observatory represents a urban supersite that is suitable for the advanced study of the atmospheric circulation, the physical and optical properties of aerosols and gases, and the validation of new satellite products.

The BAQUNIN setup, both as the strategic geographic position of observation sites in environments with different levels of urbanization and as availability of outputs covering different aspects of the atmospheric characterization, could be exported to other cities for the in-depth study of PBL and air quality.

Plans to expand the number of measurement sites hosting BAQUNIN instruments are in the early stages of development, taking into consideration other strategic locations that can be used as a reference point and/or background for the study of pollution and for the characterization of medium- and long-range aerosol advection, as well as for the cal/val of satellite products in environmental conditions (e.g., surface reflectance, land coverage, and orography).

The number of instruments managed in the BAQUNIN framework is constantly increasing, aiming at filling current measurement gaps. In particular, the upgrade of instruments is already planned to allow measuring the atmospheric content of aerosols also at nighttime, such as the addition of a Prede-POM for moon measurements. Moon measurements with the Brewer are also foreseen, to provide O_3 and NO_2 TC nighttime amounts and, possibly, AOD. New products, such as cloud top/bottom from MLW lidar and cloud fraction from all-sky cameras, are also under development and will be released shortly. Furthermore, the installation of instruments capable of filling the current lack of observations (e.g., vertical profile of temperature and CO_2, vertical profiles of wind velocity at higher altitudes, aerosol chemistry, and surface absorbent/diffusing properties of the aerosols, among others) is being evaluated. The atmospheric dispersion and the role of atmospheric stability on the short-term transport of a continuous-release passive scalar plume in three different convective boundary layer regimes will be investigated numerically, by conducting WRF simulations on specific known cases of pollution leaks caused by fire incidents.

The availability of long time series will permit to investigate the intensity of UHI and UPI, how their strength and frequency vary over time, also developing possible mitigation scenarios employing nature-based solutions.

Furthermore, BAQUNIN represents an optimal opportunity for testing synergistic retrieval approaches, thanks to the exploitation of the complex instrumental suite. The policy of free products dissemination indeed constitutes a model to be exported and replicated at other observatories.

BAQUNIN encourages researchers to participate in projects, field campaigns, and collaborations or to propose new lines of research. Furthermore, the APL site can host instruments belonging to other national and international research entities for intensive measurement campaigns or for long-term studies. The BAQUNIN consortium plans to continue and expand collaborations with universities, government agencies, and research institutions.

Acknowledgments. The authors dedicate this work to the memory of their colleague and friend Marco Cacciani. With scientific curiosity, passion, and enthusiasm, he dedicated himself to the establishment and development of the BAQUNIN supersite. This research has been funded by ESA BAQUNIN Contract 4000126749/19/I-NS. PGN is a bilateral project supported with funding from NASA and ESA.

The authors thank the technicians (G. Esposito, M. Montagnoli, M. Giusto, and T. Sargolini) of CNR-IIA for maintaining the instruments at the CNR-IIA site and providing the products useful for BAQUNIN aims. The authors gratefully acknowledge ARPA Lazio, Fondazione Osservatorio Milano Duomo, and AERONET for providing the atmospheric data used in this work. We are also grateful to the National Institute for Nuclear Physics (INFN) Computing Systems and Networks Service for the valuable support in the design and development of the database infrastructure.

Data availability statement. All data used in the present study are openly available from the websites of BAQUNIN (www.baqunin.eu/) and ARPA Lazio (www.arpalazio.it/) or can be requested from OMD (www.fondazioneomd.it/home-eng) and CNR-IIA (https://en.iia.cnr.it/).

References

Ansmann, A., M. Riebesell, U. Wandinger, C. Weitkamp, E. Voss, W. Lahmann, and W. Michaelis, 1992: Combined Raman elastic-backscatter lidar for vertical profiling of moisture, aerosol extinction, backscatter, and lidar ratio. *Appl. Phys.*, **55B**, 18–28, https://doi.org/10.1007/BF00348608.

Azouzoute, A., A. A. Merrouni, E. G. Bennouga, and A. Gennioui, 2019: Accuracy measurement of pyranometer vs reference cell for PV resource assessment. *Energy Procedia*, **157**, 1202–1209, https://doi.org/10.1016/j.egypro.2018.11.286.

Baklanov, A. A., and R. B. Nuterman, 2009: Multi-scale atmospheric environment modelling for urban areas. *Adv. Appl. Sci. Res.*, **3**, 53–57, https://doi.org/10.5194/asr-3-53-2009.

Berezin, I. A., and Coauthors, 2017: Error analysis of integrated water vapor measured by CIMEL photometer. *Izv. Atmos. Oceanic Phys.*, **53**, 58–64, https://doi.org/10.1134/S0001433817010030.

Bonn, B., and Coauthors, 2018: Impact of vegetative emissions on urban ozone and biogenic secondary organic aerosol: Box model study for Berlin, Germany. *J. Cleaner Prod.*, **176**, 827–841, https://doi.org/10.1016/j.jclepro.2017.12.164.

Campanelli, M., and Coauthors, 2018: The QUATRAM Campaign: Quality and Traceabiliy of Atmospheric Aerosol Measurements. *2018 WMO/CIMO Technical Conf. on Meteorological and Environmental Instruments and Methods of Observation*, Amsterdam, Netherlands, WMO/CIMO, 132.

——, and Coauthors, 2021: A wide-ranging investigation of the COVID-19 lockdown effects on the atmospheric composition in various Italian urban sites (AER–LOCUS). *Urban Climate*, **39**, 100954, https://doi.org/10.1016/j.uclim.2021.100954.

Camuffo, D., 2010: The role of temperature and moisture. Basic environmental mechanisms affecting cultural heritage: Understanding deterioration mechanisms for conservation purposes, COST Action D42, 9–30.

Casadio, S., A. Dehn, T. Fehr, and B. R. Bojkov, 2013: The Atmospheric Composition Validation and Evolution workshop (ACVE2013)—Recommendations. *Ann. Geophys.*, **56**, 6535, https://doi.org/10.4401/ag-6535.

Casale, G. R., A. M. Siani, H. Diémoz, G. Agnesod, M. Pedone, and A. Colosimo, 2016: Modelli di previsione dell'indice ultravioletto (UVI). *VI Convegno Nazionale*, Alessandria, Italy, ARPA.

Cattrall, C., J. Reagan, K. Thome, and O. Dubovik, 2005: Variability of aerosol and spectral lidar and backscatter and extinction ratios of key aerosol types derived from selected Aerosol Robotic Network locations. *J. Geophys. Res.*, **110**, D10S11, https://doi.org/10.1029/2004JD005124.

Chen, F., and Coauthors, 2011: The integrated WRF/urban modelling system: Development, evaluation, and applications to urban environmental problems. *Int. J. Climatol.*, **31**, 273–288, https://doi.org/10.1002/joc.2158.

Ciardini, V., L. Caporaso, R. Sozzi, I. Petenko, A. Bolignano, M. Morelli, D. Melas, and S. Argentini, 2019: Interconnections of the urban heat island with the spatial and temporal micrometeorological variability in Rome. *Urban Climate*, **29**, 100493, https://doi.org/10.1016/j.uclim.2019.100493.

Crutzen, P. J., 2004: New directions: The growing urban heat and pollution "island" effect—Impact on chemistry and climate. *Atmos. Environ.*, **38**, 3539–3540, https://doi.org/10.1016/j.atmosenv.2004.03.032.

Di Bernardino, A., and Coauthors, 2021a: On the effect of sea breeze regime on aerosol and gases properties in the urban area of Rome, Italy. *Urban Climate*, **37**, 100842, https://doi.org/10.1016/j.uclim.2021.100842.

——, and Coauthors, 2021b: Impact of synoptic meteorological conditions on air quality in three different case studies in Rome, Italy. *Atmos. Pollut. Res.*, **12**, 76–88, https://doi.org/10.1016/j.apr.2021.02.019.

Diémoz, H., and Coauthors, 2021: Advanced NO_2 retrieval technique for the Brewer spectrophotometer applied to the 20-year record in Rome, Italy. *Earth Syst. Sci. Data*, **13**, 4929–4950, https://doi.org/10.5194/essd-13-4929-2021.

Di Girolamo, P., P. F. Ambrico, A. Amodeo, A. Boselli, G. Pappalardo, and N. Spinelli, 1999: Aerosol observations by lidar in the nocturnal boundary layer. *Appl. Opt.*, **38**, 4585–4595, https://doi.org/10.1364/AO.38.004585.

Fountoulakis, I., H. Diémoz, A. M. Siani, A. di Sarra, D. Meloni, and D. M. Sferlazzo, 2021: Variability and trends in surface solar spectral ultraviolet irradiance in Italy: On the influence of geopotential height and lower-stratospheric ozone. *Atmos. Chem. Phys.*, **21**, 18689–18705, https://doi.org/10.5194/acp-21-18689-2021.

Freudenthaler, V., H. Linné, A. Chaikovski, D. Rabus, and S. Groß, 2018: EARLINET lidar quality assurance tools. *Atmos. Meas. Tech. Discuss.*, https://doi.org/10.5194/amt-2017-395.

Giles, D. M., and Coauthors, 2019: Advancements in the Aerosol Robotic Network (AERONET) version 3 database—Automated near-real-time quality control algorithm with improved cloud screening for sun photometer aerosol optical depth (AOD) measurements. *Atmos. Meas. Tech.*, **12**, 169–209, https://doi.org/10.5194/amt-12-169-2019.

Gobbi, G. P., F. Angelini, F. Barnaba, F. Costabile, J. M. Baldasano, S. Basart, R. Sozzi, and A. Bolignano, 2013: Changes in particulate matter physical properties during Saharan advections over Rome (Italy): A four-year study, 2001–2004. *Atmos. Chem. Phys.*, **13**, 7395–7404, https://doi.org/10.5194/acp-13-7395-2013.

Hatakka, J., and Coauthors, 2003: Overview of the atmospheric research activities and results at Pallas GAW station. *Boreal Environ. Res.*, **8**, 365–384, www.borenv.net/BER/archive/pdfs/ber8/ber8-365.pdf.

Herman, J., R. Evans, A. Cede, N. Abuhassan, I. Petropavlovskikh, and G. McConville, 2015: Comparison of ozone retrievals from the Pandora spectrometer system and Dobson spectrophotometer in Boulder, Colorado. *Atmos. Meas. Tech.*, **8**, 3407–3418, https://doi.org/10.5194/amt-8-3407-2015.

Huang, C., J. Yang, N. Clinton, L. Yu, H. Huang, I. Dronova, and J. Jin, 2021: Mapping the maximum extents of urban green spaces in 1039 cities using dense satellite images. *Environ. Res. Lett.*, **16**, 064072, https://doi.org/10.1088/1748-9326/ac03dc.

Illingworth, A. J., and Coauthors, 2015: The EarthCARE satellite: The next step forward in global measurements of clouds, aerosols, precipitation, and radiation. *Bull. Amer. Meteor. Soc.*, **96**, 1311–1332, https://doi.org/10.1175/BAMS-D-12-00227.1.

Kaimal, J. C., and J. E. Gaynor, 1983: The Boulder Atmospheric Observatory. *J. Appl. Meteor. Climatol.*, **22**, 863–880, https://doi.org/10.1175/1520-0450(1983)022<0863:TBAO>2.0.CO;2.

Karl, T., and Coauthors, 2020: Studying urban climate and air quality in the Alps: The Innsbruck Atmospheric Observatory. *Bull. Amer. Meteor. Soc.*, **101**, E488–E507, https://doi.org/10.1175/BAMS-D-19-0270.1.

Klett, J. D., 1985: Lidar inversion with variable backscatter/extinction ratios. *Appl. Opt.*, **24**, 1638–1643, https://doi.org/10.1364/AO.24.001638.

Kudo, R., and Coauthors, 2021: Optimal use of the Prede POM sky radiometer for aerosol, water vapor, and ozone retrievals. *Atmos. Meas. Tech.*, **14**, 3395–3426, https://doi.org/10.5194/amt-14-3395-2021.

Madonna, F., and Coauthors, 2011: CIAO: The CNR-IMAA advanced observatory for atmospheric research. *Atmos. Meas. Tech.*, **4**, 1191–1208, https://doi.org/10.5194/amt-4-1191-2011.

Mallone, S., S. Stafoggia, A. Faustini, G. P. Gobbi, A. Marconi, and F. Forastiere, 2011: Saharan dust and associations between particulate matter and daily mortality in Rome, Italy. *Environ. Health Perspect.*, **119**, 1409–1414, https://doi.org/10.1289/ehp.1003026.

Mastrantonio, G., and G. Fiocco, 1982: Accuracy of wind velocity determinations with Doppler sodars. *J. Appl. Meteor.*, **21**, 823–830, https://doi.org/10.1175/1520-0450(1982)021<0823:AOWVDW>2.0.CO;2.

——, S. Argentini, and A. Viola, 1994: A new PC-based real time system to analyze sodar-echoes. *Italian Research on Antarctic Atmosphere*, M. Colacino, G. Giovanelli, and L. Stefanutti, Eds., Vol. 45, Italian Physical Society, 227–235.

Mielke, B., 2005: Analog + photon counting. Licel Tech. Note, 10 pp., http://licel.com/manuals/analogpc.pdf.

Müller, D., A. Ansmann, I. Mattis, M. Tesche, U. Wandinger, D. Althausen, and G. Pisani, 2007: Aerosol-type-dependent lidar ratios observed with Raman lidar. *J. Geophys. Res.*, **112**, D16202, https://doi.org/10.1029/2006JD008292.

Nahian, M. R., and Coauthors, 2020: Complex meteorology over a complex mining facility: Assessment of topography, land use, and grid spacing modifications in WRF. *J. Appl. Meteor. Climatol.*, **59**, 769–789, https://doi.org/10.1175/JAMC-D-19-0213.1.

Nakajima, T., and Coauthors, 2020: An overview of and issues with sky radiometer technology and SKYNET. *Atmos. Meas. Tech.*, **13**, 4195–4218, https://doi.org/10.5194/amt-13-4195-2020.

Nicolae, D., J. Vasilescu, E. Carstea, K. Stebel, and F. Prata, 2010: Romanian Atmospheric Research 3D Observatory: Synergy of instruments. *Rom. Rep. Phys.*, **62**, 838–853, www.rrp.infim.ro/2010_62_4/art17Doina.pdf.

Nuruzzaman, M., 2015: Urban heat island: Causes, effects and mitigation measures—A review. *Int. J. Environ. Monit. Anal.*, **3**, 67–73, https://doi.org/10.11648/j.ijema.20150302.15.

Park, M.-S., S.-H. Park, J.-H. Chae, M.-H. Choi, Y. Song, M. Kang, and J.-W. Rohand, 2017: High-resolution urban observation network for user-specific meteorological information service in the Seoul Metropolitan Area, South Korea. *Atmos. Meas. Tech.*, **10**, 1575–1594, https://doi.org/10.5194/amt-10-1575-2017.

Peel, M. C., B. L. Finlayson, and T. A. McMahon, 2007: Updated world map of the Köppen-Geiger climate classification. *Hydrol. Earth Syst. Sci.*, **11**, 1633–1644, https://doi.org/10.5194/hess-11-1633-2007.

Pelliccioni, P., and Coauthors, 2020: Integrated evaluation of indoor particulate exposure: The VIEPI project. *Sustainability*, **12**, 9758, https://doi.org/10.3390/su12229758.

Petenko, I., G. Mastrantonio, A. Viola, S. Argentini, L. Coniglio, P. Monti, and G. Leuzzi, 2011: Local circulation diurnal patterns and their relationship with large-scale flows in a coastal area of the Tyrrhenian Sea. *Bound.-Layer Meteor.*, **139**, 353–366, https://doi.org/10.1007/s10546-010-9577-x.

Pichelli, E., R. Ferretti, M. Cacciani, A. M. Siani, V. Ciardini, and T. Di Iorio, 2014: The role of urban boundary layer investigated with high-resolution models and ground-based observations in Rome area: A step towards understanding parameterization potentialities. *Atmos. Meas. Tech.*, **7**, 315–332, https://doi.org/10.5194/amt-7-315-2014.

Rao, M. P., S. Casadio, G. Fiocco, M. Cacciani, A. Di Sarra, D. Fua, and P. Castracane, 2002: Estimation of atmospheric water vapour flux profiles in the nocturnal unstable urban boundary layer with Doppler sodar and Raman lidar. *Bound.-Layer Meteor.*, **102**, 39–62, https://doi.org/10.1023/A:1012794731389.

——, P. Castracane, S. Casadio, D. Fua, and G. Fiocco, 2004: Observations of atmospheric solitary waves in the urban boundary layer. *Bound.-Layer Meteor.*, **111**, 85–108, https://doi.org/10.1023/B:BOUN.0000010998.10262.e2.

Siani, A. M., F. Frasca, F. Scarlatti, A. Religi, H. Diémoz, G. R. Casale, M. Pedone, and V. Savastiouk, 2018: Examination on total ozone column retrievals by Brewer spectrophotometry using different processing software. *Atmos. Meas. Tech.*, **11**, 5105–5123, https://doi.org/10.5194/amt-11-5105-2018.

Skamarock, W. C., and Coauthors, 2008: A description of the Advanced Research WRF version 3. NCAR Tech. Note NCAR/TN-475+STR, 113 pp., https://doi.org/10.5065/D68S4MVH.

Sterzel, T., M. K. Lüdeke, C. Walther, M. T. Kok, D. Sietz, and P. L. Lucas, 2020: Typology of coastal urban vulnerability under rapid urbanization. *PLOS ONE*, **15**, e0220936, https://doi.org/10.1371/journal.pone.0220936.

Stevens, B., and Coauthors, 2016: The Barbados Cloud Observatory: Anchoring investigations of clouds and circulation on the edge of the ITCZ. *Bull. Amer. Meteor. Soc.*, **97**, 787–801, https://doi.org/10.1175/BAMS-D-14-00247.1.

Struckmeier, C., F. Drewnick, F. Fachinger, G. P. Gobbi, and S. Borrmann, 2016: Atmospheric aerosols in Rome, Italy: Sources, dynamics and spatial variations during two seasons. *Atmos. Chem. Phys.*, **16**, 15,277–15,299, https://doi.org/10.5194/acp-16-15277-2016.

Sugiura, K., and Coauthors, 2011: Supersite as a common platform for multi-observations in Alaska for a collaborative framework between JAMSTEC and IARC. *JAMSTEC Rep. Res. Dev.*, **12**, 61–69, https://doi.org/10.5918/jamstecr.12.61.

Suto, H., and Coauthors, 2021: Thermal And Near-infrared Sensor for carbon Observation Fourier Transform Spectrometer-2 (TANSO-FTS-2) on the Greenhouse gases Observing Satellite-2 (GOSAT-2) during its first year in orbit. *Atmos. Meas. Tech.*, **14**, 2013–2039, https://doi.org/10.5194/amt-14-2013-2021.

Tanaka, K., and Coauthors, 2018: First year on-orbit calibration activities of SGLI on GCOM-C satellite. *Proc. SPIE*, **10781**, 107810Q, https://doi.org/10.1117/12.2324703.

United Nations, 2019: Department of economic and social affairs: Population dynamics. United Nations, https://population.un.org/wpp/.

Veefkind, J. P., and Coauthors, 2012: TROPOMI on the ESA Sentinel-5 Precursor: A GMES mission for global observations of the atmospheric composition for climate, air quality and ozone layer applications. *Remote Sens. Environ.*, **120**, 70–83, https://doi.org/10.1016/j.rse.2011.09.027.

Verhoelst, T., and Coauthors, 2021: Ground-based validation of the Copernicus Sentinel-5P TROPOMI NO_2 measurements with the NDACC ZSL-DOAS, MAX-DOAS and Pandonia global networks. *Atmos. Meas. Tech.*, **14**, 481–510, https://doi.org/10.5194/amt-14-481-2021.

Wolfe, D. E., and R. J. Lataitis, 2018: Boulder Atmospheric Observatory: 1977–2016: The end of an era and lessons learned. *Bull. Amer. Meteor. Soc.*, **99**, 1345–1358, https://doi.org/10.1175/BAMS-D-17-0054.1.

Zhang, Y., and Coauthors, 2019: Six-year source apportionment of submicron organic aerosols from near-continuous highly time-resolved measurements at SIRTA (Paris area, France). *Atmos. Chem. Phys.*, **19**, 14755–14776, https://doi.org/10.5194/acp-19-14755-2019.